

Establishment of a Bernard-Soulier syndrome model in zebrafish

Qing Lin,^{1,2*} Riyang Zhou,^{1,2*} Panpan Meng,^{2*} Liangliang Wu,² Lian Yang,² Wenyu Liu,² Jiaye Wu,² Yuhuan Cheng,¹ Linjuan Shi¹ and Yiyue Zhang^{1,2}

¹Key Laboratory of Zebrafish Modeling and Drug Screening for Human Diseases of Guangdong Higher Education Institutes, Department of Developmental Biology, School of Basic Medical Sciences, Southern Medical University and ²Division of Cell, Developmental and Integrative Biology, School of Medicine, South China University of Technology, Guangzhou, China

*QL, RZ and PM contributed equally as co-first authors.

Correspondence:

Yiyue Zhang
mczhangyy@scut.edu.cn

Received: March 30, 2021.

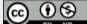
Accepted: August 6, 2021.

Prepublished: August 19, 2021.

<https://doi.org/10.3324/haematol.2021.278893>

©2022 Ferrata Storti Foundation

Haematologica material is published under a CC

BY-NC license 

Abstract

Platelets play an essential role in thrombosis and hemostasis. Abnormal hemostasis can cause spontaneous or severe post-traumatic bleeding. Bernard-Soulier syndrome (BSS) is a rare inherited bleeding disorder caused by a complete quantitative deficiency in the GPIb-IX-V complex. Multiple mutations in *GP9* lead to the clinical manifestations of BSS. Understanding the roles and underlying mechanisms of *GP9* in thrombopoiesis and establishing a proper animal model of BSS would be valuable to understand the disease pathogenesis and to improve its medical management. Here, by using CRISPR-Cas9 technology, we created a zebrafish *gp9*^{SMU15} mutant to model human BSS. Disruption of zebrafish *gp9* led to thrombocytopenia and a pronounced bleeding tendency, as well as an abnormal expansion of progenitor cells. The *gp9*^{SMU15} zebrafish can be used as a BSS animal model as the roles of *GP9* in thrombopoiesis are highly conserved from zebrafish to mammals. Utilizing the BSS model, we verified the clinical *GP9* mutations by *in vivo* functional assay and tested clinical drugs for their ability to increase platelets. Thus, the inherited BSS zebrafish model could be of benefit for *in vivo* verification of patient-derived *GP9* variants of uncertain significance and for the development of potential therapeutic strategies for BSS.

Introduction

Platelets play an essential role in thrombosis and hemostasis. Without nuclei, they are the smallest formed elements of the blood in mammals, and are produced from giant polyploid precursors, the megakaryocytes.¹ Megakaryocytes differentiate from hematopoietic stem cells in the hematopoietic sites (bone marrow, yolk sac, fetal liver and spleen). It is well accepted that hematopoietic stem cells give rise to megakaryocyte-erythrocyte progenitors in the first instance, and these progenitors commit to both erythroid and megakaryocytic lineage cells.²⁻⁴ During thrombopoiesis, megakaryocytes then arise from committed megakaryocytic precursors, undergo several cycles of endomitosis to become polyploid and release platelets as cell fragments into the bloodstream.⁵ When a blood vessel ruptures, adherent platelets become activated and initiate the platelet aggregation process, so the circulating platelets adhere to different components of vascular sub-endothelial structures to stop the bleeding.³

Functional platelets require a series of platelet membrane receptors properly expressed, as these receptors are es-

sential for platelet adhesion to form clots on the damaged vessel wall and trigger transmembrane signaling leading to cell aggregation and activation. The glycoprotein Ib-IX-V complex (GPIb-IX-V), expressed in platelets and megakaryocytes, belongs to the leucine-rich repeat family of membrane proteins. The complex consists of four distinct transmembrane polypeptide subunits,⁶ of which GPIb α , GPIb β , and GPIX are all necessary for efficient biosynthesis of the receptor, whereas GPV is more loosely associated.^{7,8} When blood vessels rupture causing bleeding, the GPIb-IX-V complex mediates platelet attachment to the sites of blood vessel wall injury and activates the platelets.⁹ Bernard-Soulier syndrome (BSS), a rare autosomal recessively inherited bleeding disorder also known as hemorrhagic thrombocytopenic dystrophy,⁷⁻⁹ is caused by quantitative or qualitative defects within the membrane GPIb-IX-V complex.⁶ The syndrome is characterized by thrombocytopenia, giant platelets with the absence of platelet aggregation in response to ristocetin, and a range of sometimes life-threatening mucocutaneous bleeding disorders.^{7,9} Mutations in *GP1BA* (GPIb α), *GP1BB* (GPIb β), and *GP9* (GPIX) have all been reported in BSS patients,¹⁰

with the reported mutation frequency being higher in *GP9* than in the other two genes in a study of 211 BSS families.¹⁰ GPIX is a subunit of the platelet membrane glycoprotein complex, and multiple point mutations in the *GP9* gene are reported to be associated with BSS in patients.^{10,11} Several *GP9* point mutations, such as *GP9* 70T>C and *GP9* 182A>G, have been reported to affect protein conformation and consequently attenuate the GPIIb-IX-V complex component expression, but there is still a lack of *in vivo* functional evidence on whether these mutations affect thrombocytes.^{10,12-15} Disruption of GPIX in mice results in thrombocytopenia with giant platelets and prolonged bleeding phenotypes similar to human BSS, while intra-uterine embryogenesis makes mice difficult to manipulate during early developmental stages.¹⁶ Whether and how *GP9* participates in the regulation of embryonic thrombocyte development remains incompletely known.

Zebrafish (*Danio rerio*) have been used as powerful vertebrate models for developmental biology and for modeling many human diseases. Their high fecundity, external development and their optical transparency during early development facilitate high-throughput genetic and small-molecule screening, especially for *in vivo* phenotype fast-reading in early developmental stages. Importantly, thrombocytes in early vertebrates are equivalent to mammalian platelets in functional and regulatory terms.^{17,18} Thrombocytopoiesis has been described in zebrafish and has demonstrated conservation of regulatory factors and similar developmental processes as those in mammals.^{19,20} Thrombocyte disorders including congenital amegakaryocytic thrombocytopenia, inherited thrombocytopenia, essential thrombocythemia and several platelet functional disorders have been modeled successfully in zebrafish.²¹⁻²⁵ In addition, thrombocytic lineage-specific transgenic reporter strains of zebrafish are available, such as the *Tg(cd41:eGFP)* and *Tg(mpl:eGFP)* lines.^{19,21} Thrombocyte function can be detected by the efficiency of clotting, measured as the time to occlusion or the thrombus surface area, both having been well-established in zebrafish.^{21,26} As multiple mutations in *GP9* are associated with clinical manifestations of BSS, understanding the functions and underlying mechanisms of *GP9* in thrombocytopoiesis and establishing a proper zebrafish model of BSS would be valuable to understand the disease pathogenesis and to verify the clinical significance of patient-derived *GP9* variants.

In the current study, we targeted the *gp9* gene using CRISPR-Cas9 technology to generate an inherited BSS zebrafish model. The *gp9*^{SMU15} zebrafish modeled BSS well, as it displayed thrombocytopenia from early development to adult stage, thrombocytic progenitor expansion in adult hematopoiesis, and exhibited bleeding disorders. We further demonstrated that human *GP9* mirrored the thrombocyte phenotypes in the zebrafish model, and pa-

tient-derived *GP9*^{70T>C} and *GP9*^{182A>G} mutations are thrombocytopoietic deficient mutations responsible for human BSS. Moreover, we found that recombinant human thrombopoietin (rhTPO), used clinically for promoting thrombocytopoiesis, was also effective for relapsing BSS thrombocytopenia phenotypes in the model. Interestingly, we found that decitabine, used for treating leukemia and idiopathic thrombocytopenia purpura in the clinic, could also effectively alleviate thrombocytopenia in BSS zebrafish. Thus, *gp9*^{SMU15} zebrafish could serve as an ideal model for understanding the deficiency of thrombocytopoiesis and hemostasis associated with BSS, and it could be applied as a useful tool for fast clarifying human patient-derived *GP9* variants of unknown clinical significance, as well as for the development of therapeutic strategies for BSS.

Methods

Generation of *gp9*^{SMU15} mutant lines

We generated *gp9*^{SMU15} mutants using the CRISPR/Cas9 method. The zebrafish *gp9* target within exon 2 is 5'-GGGCAAAGTCACGCACCTGC-3'. *gp9* guide RNA was transcribed *in vitro* by using mMACHINE kit (Ambion). We generated *gp9* mutants by injecting one-cell stage embryos with Cas9 protein (EnGen Cas9 NLS, NEB) and gRNA. F0 fish were crossed with wild-type (WT) fish to produce F1 progeny, which were then genotyped and sequenced to identify the inheritable mutation. We acquired the main frameshift mutations with the deletion of 17 bp (F1). We crossed the heterozygotes F1 *gp9*^{SMU15/+} to generate homozygous mutant F2 *gp9*^{SMU15}. All work involving zebrafish was reviewed and approved by the Animal Ethics Committee or the Animal Research Advisory Committee of Southern Medical University and South China University of Technology

Analysis of thrombocyte function

We monitored the time to stop bleeding or the bleeding area size in adult zebrafish and the time to occlusion in zebrafish larvae after injury. Comparable cuts were made in WT siblings and *gp9*^{SMU15} mutants with a scalpel blade at the junction region between the torso and the tail fin to destroy the vessels near the tail part; the cuts were performed in a single-blind manner to exclude the subjective factor of operation, and the fish were genotyped after the injury. The time to stop bleeding (the time the injury was made to the time the bleeding stopped) was measured under a microscope and recorded by a video camera. Sodium hydroxide (NaOH) treatment to induce gill bleeding was performed as previously described with some modifications.^{27,28} We placed zebrafish in a glass dish containing 15 mL of 20 mM NaOH solution, and the process was recorded under a microscope (Carl Zeiss Meditec AG, Jena,

Germany). FeCl₃ treatment was performed as previously described with some modifications.^{26,29} In detail, 6-day post-fertilization (dpf) larvae, with various genotypes *Tg(cd41:eGFP);WT* siblings and *Tg(cd41:eGFP);gp9^{SMU15}* were

immobilized in 0.8% low-melt agarose gel and 0.02% anesthetic tricaine (Sigma-Aldrich). A drop (2.5 μL) of 1% FeCl₃ was placed on the tail region. From the time the first drop appeared on the tail region to the accumulation of the

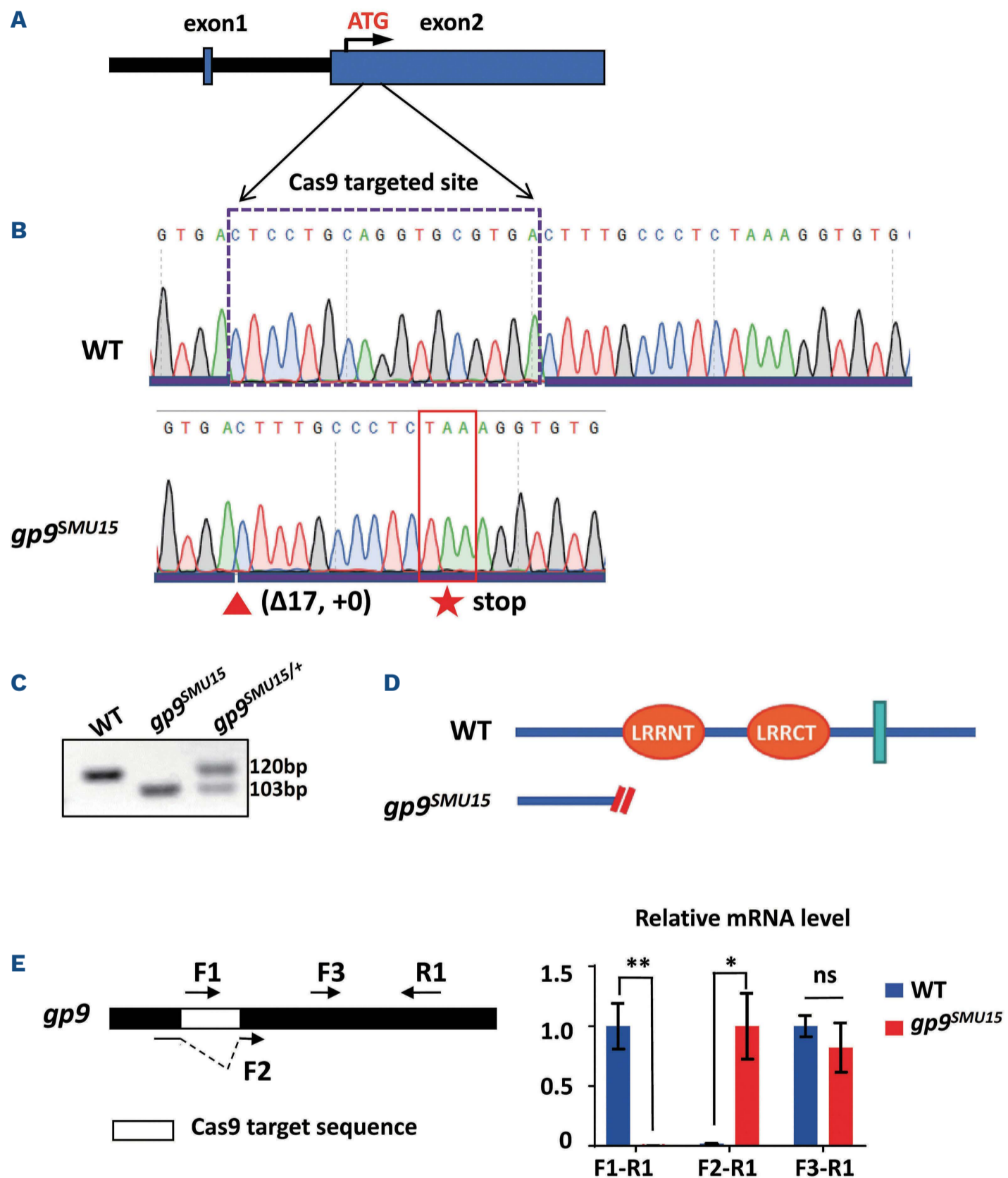


Figure 1. Generation and characterization of *gp9^{SMU15}* zebrafish using CRISPR/Cas9. (A) The zebrafish *gp9* gene structure. The start coding region is shown with ATG. The targeting sequence aimed at the coding region is shown in the purple dashed box. (B) Sanger sequencing identified the wild-type (WT) sequence (top) and 17-bp deletion (red arrowhead) in *gp9^{SMU15}*. Frameshift mutation of *gp9* creates premature stop codons indicated with the red asterisk. (C) Agarose gel pictures of the polymerase chain reaction product from WT, mutant, and heterozygote zebrafish. Lane 1: the wild type bands; lane 2: the mutant bands; lanes 3: the heterozygote bands. (D) Gp9 protein structures in WT and mutant fish. The Gp9 protein analyzed with the SMART program contains one leucine-rich repeat N-terminal (LRRNT) domain, one leucine-rich repeat C-terminal (LRRCT) domain and one transmembrane domain. Orange ovals indicate a LRRNT or LRRCT domain, the green box indicates the transmembrane domain. Red slashes indicate the premature stop of Gp9 protein. (E) *gp9^{Δ17,+0}* mutated transcripts generated in *gp9^{SMU15}* mutants. Primer pairs F1 (wt_FP) F2 (mut_FP) F3 (common_FP) and R1 (common_RP) were utilized for detecting the WT form and *gp9^{Δ17,+0}* form, respectively. Statistical significance was determined using a two-sample Student *t*-test, $n \geq 10$ per group, data were combined from four biological replicates, mean \pm standard error of mean. ** $P < 0.01$; * $P < 0.05$; ns: not significant.

thrombocytes at the injury site, the time to occlusion was measured at the microscopic stage monitored by a fluorescence microscope.

Drug treatment

Tg(cd41:eGFP) sibling and *Tg(cd41:eGFP);gp9^{SMU15}* transgenic

mutant zebrafish were utilized. Embryos were soaked into egg water containing drugs in appropriate concentration at 36 hours post-fertilization (hpf) using 12-well plates and scored at 4 dpf by counting the *cd41:eGFP^{high}*-labeled thrombocytes to determine whether drugs were effective. Fifteen embryos were put in each well with a volume of 3

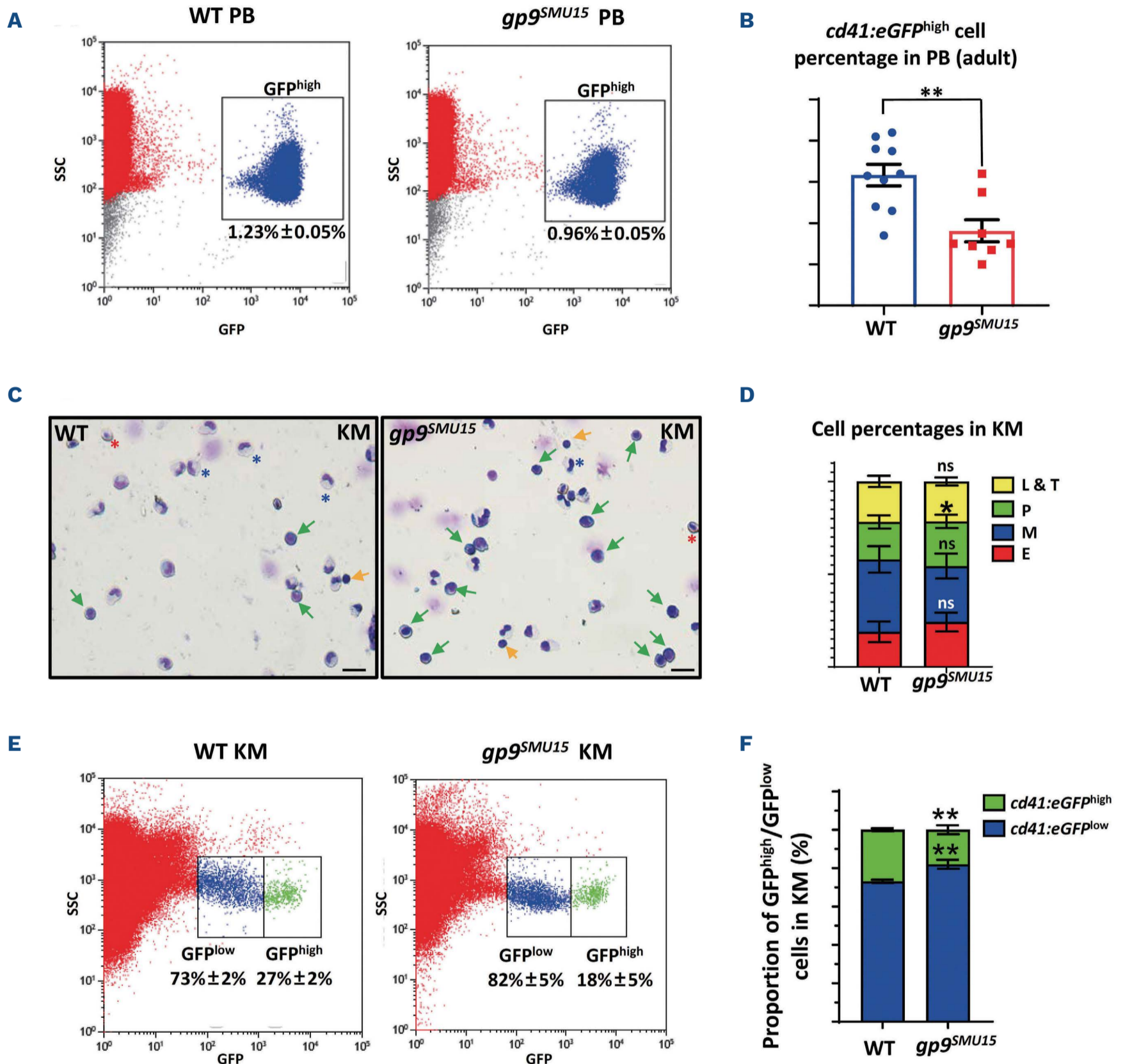


Figure 2. *gp9^{SMU15}* adult fish display thrombocytopenia and abnormal precursor expansion. (A) Flow cytometry analysis of peripheral blood (PB) cells in wild-type (WT) and *gp9^{SMU15}* fish. FITC was directly proportional to 488-GFP cells and side scatter (SSC) was indicative of cellular granularity. (B) Percentage of *cd41:eGFP⁺* thrombocytes in PB determined by flow cytometry (Student *t*-test, *n*=6; mean ± standard error of mean [SEM]; ns: not significant; **P*<0.05). (C) May-Grünwald-Giemsa staining of kidney marrow (KM) cells in WT and *gp9^{SMU15}* fish. The scale bar represents 20 μm. Arrowheads are colored yellow for lymphocytes or thrombocytes and green for precursors. Asterisks are colored blue for myelomonocytes and red for erythrocytes. (D) Blood cell counts of WT and *gp9^{SMU15}* KM by May-Grünwald-Giemsa staining. L&T: lymphocytes and thrombocytes; P: precursors; M: myelomonocytes; E: erythrocytes. (Student *t*-test, *n*=6; mean ± SEM; ns: not significant; **P*<0.05). (E) Flow cytometry analysis of KM cells in WT and *gp9^{SMU15}* fish. FITC was directly proportional to 488-GFP cells and SSC was indicative of cellular granularity. (F) Percentage of *cd41:eGFP^{low}* and *cd41:eGFP^{high}* thrombocytes in KM cells determined by flow cytometry (Student *t*-test, *n*=6; mean ± SEM; ns: not significant; ***P*<0.01).

mL solution. To obtain a proper working concentration of rhTPO (rhTPO injection; 3SBIOINC, Shenyang, China) and decitabine (Selleck S1200; Selleck, Houston, TX, USA), we treated 1.5-dpf WT embryos with gradient concentrations of rhTPO (50, 100 and 500 U/mL) or decitabine (10, 20, 50 and 100 μ M) until 4 dpf to see whether zebrafish thrombocytes could respond to the concentrations. Doses of 100 U/mL rhTPO and 20 μ M of decitabine were chosen as the concentrations that could elevate WT thrombocytes efficiently but not cause developmental retardation in larvae.

Results

The *gp9*^{SMU15} adult fish display thrombocytopenia and hematopoietic precursor expansion

To investigate the role of *gp9* in thrombocytopoiesis, we generated a *gp9*-deficient zebrafish mutant by targeting exon 2 of the *gp9* gene using CRISPR-Cas9 technology (Figure 1A). We obtained an F0 mutant line containing *gp9* (-17 bp, +0) (Figure 1B, C), and outcrossed this line with WT zebrafish to generate F1 heterozygous and F2 homozygous progenies. The *gp9* (-17 bp, +0) mutant was predicted to encode a truncated Gp9 protein lacking the two-leucine rich repeat domains and the transmembrane domain (Figure 1D). Using quantitative real-time polymerase chain reaction to detect *gp9* mRNA, we found that the mutant fish produced only the mutated mRNA (Figure 1E). Therefore, *gp9* (-17 bp, +0) (*gp9*^{SMU15} hereafter) was predicted to be a loss-of-function mutant.

To characterize the effects of *gp9* disruption on thrombocytopoiesis in zebrafish, we determined thrombocyte numbers in *gp9*^{SMU15} mutants and their siblings by monitoring *cd41:eGFP* expression in the *Tg(cd41:eGFP)* line, as the vast majority of circulating thrombocytes could be recognized by flow cytometry analysis (FACS) with bright *cd41:GFP*^{high} fluorescence in adult fish.¹⁹ Notably, although *gp9*^{SMU15} mutants were viable and able to survive to adulthood, the *gp9*^{SMU15} adult mutants displayed thrombocytopenia as the number of circulating *cd41:eGFP*^{high} thrombocytes in adult mutants was about 78% of the number in adult WT sibling fish (Figure 2A, B). These data indicate that *gp9*^{SMU15} zebrafish displayed thrombocytopenia in the adult stage, resembling BSS in human patients. To directly examine BSS-like hematologic disorders in *gp9*^{SMU15} adult fish, kidney-marrow (KM) cells were collected from *gp9*^{SMU15} adult fish or siblings and subjected to cytological analyses and blood cell count. We found a significant expansion of the precursor cell population in adult *gp9*^{SMU15} fish (Figure 2C, D). Recent single-cell RNA-sequencing of zebrafish adult KM revealed the continuous nature of thrombocyte development,³⁰ and FACS could recognize hematopoietic stem and progenitor cells (HSPC) to differentiated thrombocytes with weak to bright *cd41:eGFP*

(*GFP*^{low} to *GFP*^{high}) fluorescence in the adult KM cells.^{19,31,32} To compare the thrombocyte population of *gp9*^{SMU15} fish with that of their WT siblings in KM, *cd41:eGFP*⁺ cells were isolated by FACS. In accordance with the cytological results (Figure 2C, D), the FACS results also showed an increase in the *cd41:eGFP*^{low} cell population from 73% in the adult WT sibling fish to 82% in adult *gp9*^{SMU15} fish (Figure 2E, F), suggesting that *gp9*^{SMU15} fish had a higher percentage of *cd41:eGFP*^{low} HSPC than had their WT siblings. The morphological analysis revealed that there were no obvious cell size changes within the *cd41:eGFP*^{low} HSPC population (Online Supplementary Figure S1A, C). However, the populations of *cd41:eGFP*^{high} thrombocytes in *gp9*^{SMU15} mutant KM and peripheral blood were both larger than those in their WT siblings (medium vs. small) (Online Supplementary Figure S1A-D). The above data demonstrate that *gp9*^{SMU15} zebrafish mutants probably have a developmental block, with expansion of larger thrombocytes and reduced small-nucleated thrombocytes in adulthood. BSS patients display increased bone marrow megakaryocytes but reduced mature platelets.³⁴ In our study, zebrafish *gp9*^{SMU15} mutants showed a similar expansion of the progenitor population but reduced circulating thrombocytes.

The *gp9*^{SMU15} mutants display impaired thrombocyte function

BSS patients generally have moderate thrombocytopenia, giant platelets and a bleeding tendency. They may suffer severe hemorrhage following injury or during surgery.³³ Under normal conditions, WT zebrafish rarely bleed severely, whereas ~21% (4/19) of *gp9*^{SMU15} mutants had blood spots on the body or near the tail fins (Figure 3A), indicating that the *gp9* mutation led to a pronounced bleeding tendency. Thrombocyte function can be assessed by the ability to stop bleeding and to clot, which has been well-established in the zebrafish model.^{21,29} By calculating the time to stop bleeding after a tail-cut injury, we found that the average time in *gp9*^{SMU15} adult mutants was ~50 s, much longer than in the WT group (~20 s) (Figure 3B, C). We also used NaOH as a substance to create chemical damage to induce gill bleeding.^{27,28} We found more severe gill bleeding in *gp9*^{SMU15} fish than in WT fish (Figure 3D, E). We then monitored the accumulation of *cd41:eGFP*^{high} thrombocytes following administration of FeCl₃ to induce an oxidative injury to the vascular endothelium,^{26,29} and found that the time to accumulation of thrombocytes at the injured venule in *gp9*^{SMU15} zebrafish larvae was significantly longer (mean \pm standard error of mean [SEM], 36.4 \pm 5.2 s) than in the WT sibling controls (mean \pm SEM, 22.2 \pm 2.4 s) (Figure 3F). Taken together, these results demonstrated that the thrombocytopenic *gp9*^{SMU15} zebrafish exhibited bleeding disorders similar to the extended clinical manifestations of clotting and prolonged bleeding time in BSS patients.

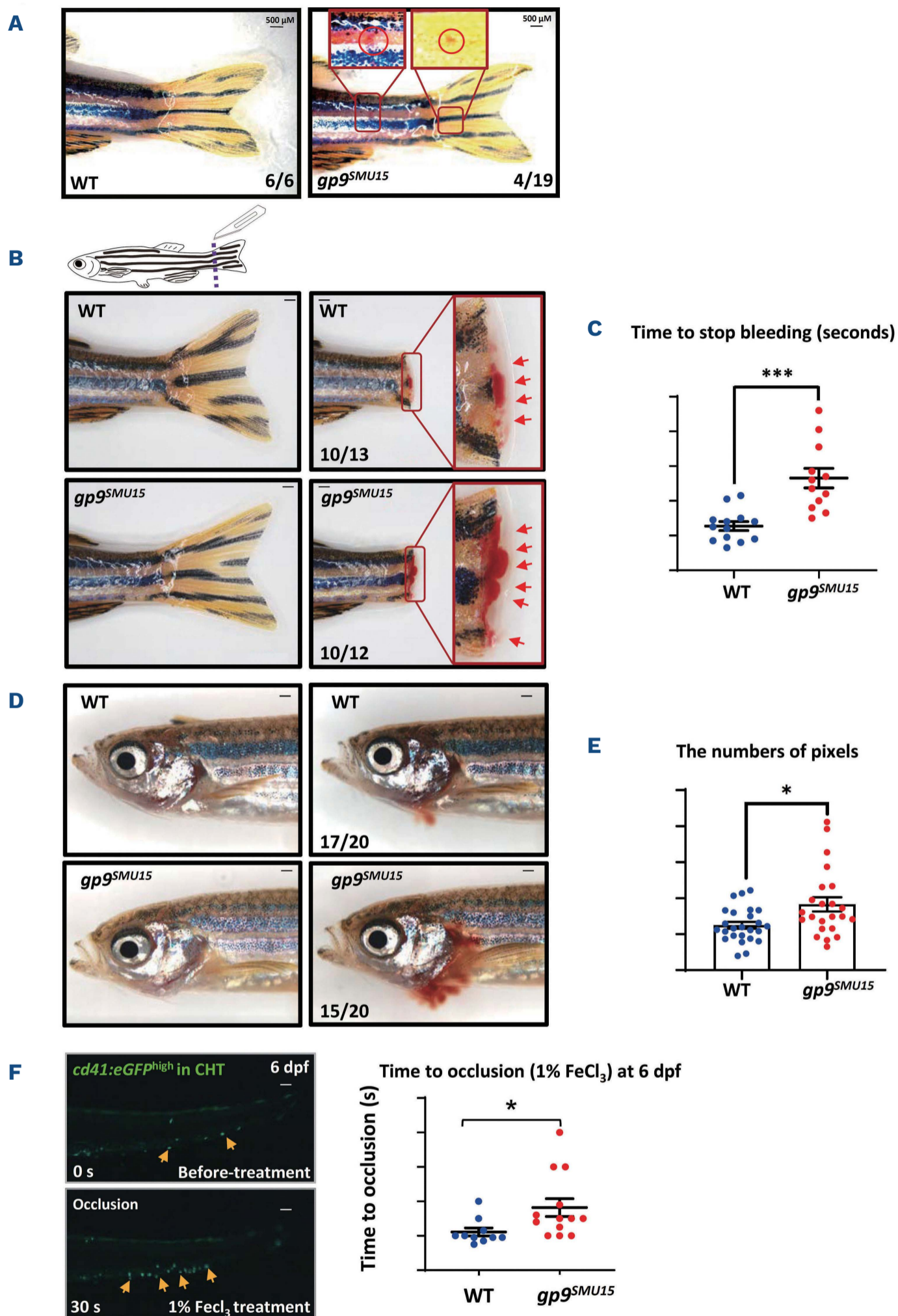


Figure 3. *gp9^{SMU15}* mutants display impaired thrombocyte function. (A–D) Clotting in adult wild-type (WT) siblings and *gp9^{SMU15}* mutants. Representative images, under normal conditions, of blood spots on the zebrafish body or near the tail fins (A). The time to stop bleeding in adult WT siblings (upper) and *gp9^{SMU15}* mutants (lower) (B). (C) Quantitative data showing the time to stop bleeding in WT and *gp9^{SMU15}* siblings (D) Representative images of gill bleeding after injury in the sibling and *gp9^{SMU15}* mutants. The representative pictures were captured at 90 s. (E) Quantitative data showing the red pixels around the gill in WT and *gp9^{SMU15}* fish. The red color pixels, indicating the extent of bleeding, were counted by Adobe photoshop CC software. (F) Zebrafish after injury induced by 1% ferric chloride: quantitative data showing the time to accumulation of thrombocytes at the injured venule. Statistical significance was determined by a two-sample Student *t*-test, $n \geq 10$, mean \pm standard error of mean, $*P < 0.05$. Scale bars: 500 μm .

The *gp9*-disruption led to thrombocytopenia in zebrafish larvae

To characterize the effects of *gp9* disruption on thrombocytopoiesis in zebrafish embryos or larvae, we determined thrombocyte numbers in *gp9*^{SMU15} mutants and their siblings by monitoring *cd41* mRNA and *cd41:eGFP* expression. In zebrafish larvae, two distinct populations of *cd41:eGFP* cells could be recognized, *cd41:eGFP*^{low} precursor and progenitor cells and the *cd41:eGFP*^{high} thrombocytes, by FACS or by whole mount observation under a fluorescence microscope.^{19,32,34} We isolated GFP⁺ cells from 3-dpf embryos by FACS, and found that the *cd41:eGFP*^{high} cell population was significantly decreased but that the *cd41:eGFP*^{low} cell population was increased in 3-dpf *gp9*^{SMU15} embryos (Figure 4A, B), suggesting that thrombocyte differentiation was affected by the *gp9* mutation. Furthermore, quantification analysis showed that, at 4 dpf, signals of *cd41:eGFP*^{high} cells in the caudal hematopoietic tissue (CHT) region were markedly reduced in *gp9*^{SMU15} mutant larvae compared with the signals from WT sibling embryos (Figure 4C, D), indicating that *gp9*^{SMU15} mutants exhibited thrombocytopenia during embryonic development. This conclusion was further supported by the downregulation of several thrombocyte-related genes, such as *cd41* and genes required for thrombocytopoiesis (*fog1* and *nfe2*) (Figure 4E). Notably, the aorta-gonad-mesonephros (AGM) *cd41:eGFP*^{low} cells, mainly represented by HSPC, were unaltered in 2-dpf *gp9*^{SMU15} mutants (Figure 4F), and *cmyb* expression was unaltered in the AGM and CHT regions (Figure 4G), suggesting that HSPC were unaffected by *gp9* mutations. Other definitive blood lineages were also unaffected, as indicated by unaltered *mpo*⁺ neutrophils at 3-dpf, β e1-globin⁺ and *O-dianisidine*⁺ erythrocytes, and *rag1*⁺ lymphocytes at 5-dpf (Online Supplementary Figure S2A-E). Furthermore, primitive blood lineages including embryonic erythroid markers (α e1-globin and *gata1*) and a primitive myeloid marker (*pu.1*) were unaffected in *gp9*^{SMU15} mutants (Online Supplementary Figure S3A-D). Taken together, these results show that *gp9*^{SMU15} mutants exhibit a lineage-specific thrombocytic deficiency without other blood lineage cells being affected.

To rule out the possibility of off-target mutations, we overexpressed Gp9-eGFP fusion protein under the control of the heat-shock promoter (*hsp:gp9-egfp*) and showed that heat-shock-induced *gp9* overexpression could protect *gp9*^{SMU15} mutants from thrombocytopenia (Online Supplementary Figure S4A-C). These data demonstrate that the loss of *gp9* function leads to thrombocytopenia in zebrafish larvae.

Thrombocytopenia in *gp9*^{SMU15} mutants is caused by reduced proliferation of thrombocyte precursors

To explain the cellular basis of the thrombocytopenia in *gp9*^{SMU15} mutants, we further explored whether thrombo-

cyte proliferation is reduced or apoptosis increased in *gp9*-deficient mutants. Thus we monitored the CHT region *cd41:eGFP* positive cell growth or death changes in the *Tg(cd41:eGFP);gp9*^{SMU15} transgenic line.³³ A 5-bromo-2'-deoxyuridine (BrdU) pulse labeling incorporation assay revealed that the percentage of BrdU-positive *cd41:eGFP*⁺ cells in total *cd41:eGFP*⁺ cells in the CHT was markedly reduced in *gp9*^{SMU15} mutants at 3 dpf, and the decreased population were BrdU-labeled *cd41:GFP*^{low} cells rather than *cd41:GFP*^{high} cells, suggesting that the proliferation of *cd41:eGFP*^{low} hematopoietic precursors or thrombocyte progenitor cells was affected by the *gp9* mutation (Figure 5A, B). To investigate the apoptosis of thrombocytes in *gp9*^{SMU15} mutants, we performed a terminal deoxynucleotidyl transferase dUTP nick-end labeling (TUNEL) assay, and found almost no *cd41:eGFP/TUNEL* double-positive cells in the CHT at 3 dpf in either WT siblings or *gp9*^{SMU15} mutants (Figure 5C), indicating that thrombocytopenia was not likely caused by apoptosis. These results demonstrated that thrombocytopenia in *gp9*^{SMU15} mutants could be mainly attributed to reduced proliferation.

Validation of the zebrafish model using human Bernard-Soulier syndrome-related GP9 mutations

The phylogenetic tree of *Gp9* suggests the evolutionary conservation from zebrafish to mammals (Online Supplementary Figure S5A). Multiple sequence alignment demonstrates the similarity of GPIX between zebrafish and mammals (Online Supplementary Figure S5B), especially in the ectodomain (with ~37% identity).³⁵

Human BSS is reported to be associated with several *GP9* mutations, such as *GP9* c.70T>C (C24R) and *GP9* c.182A>G (N61S) (Online Supplementary Figure S5B), which have been noted to change the GPIX conformation and mildly impair the protein expression of itself and the GPIB-IX-V complex at the molecular level.^{10,12,13} However, there is still a lack of functional evidence for the two mutations affecting thrombocytopoiesis in animal models. To verify the mutation's effects in models, we first studied *gp9*^{SMU15} zebrafish to see whether human *GP9* (*hsGP9*^{WT} hereafter) could rescue zebrafish BSS. We found that thrombocytopenia of zebrafish *gp9*^{SMU15} mutants could be recovered by overexpression of *hsGP9*^{WT} (Figure 6A-C), as *cd41:eGFP*^{high} thrombocyte counts in *gp9*^{SMU15} zebrafish injected with *hsGP9*^{WT} mRNA (34.2 ± 3.2 thrombocytes) increased to almost the normal level in WT siblings (34.6 ± 1.9 thrombocytes) (Figure 6B, C). These results further confirmed the functional conservation of thrombocytopoiesis in zebrafish and human *GP9*, and suggested that *gp9*^{SMU15} zebrafish could be utilized as a BSS model for fast-validating the functional significance of *hsGP9* variants. We further overexpressed the human BSS isoform *GP9*c.70T>C and c.182A>G mRNA (hereafter *hs*^{GP970T>C} and *hs*^{GP9182A>G}, respectively, as shown in Online Supplementary Figure S5A)

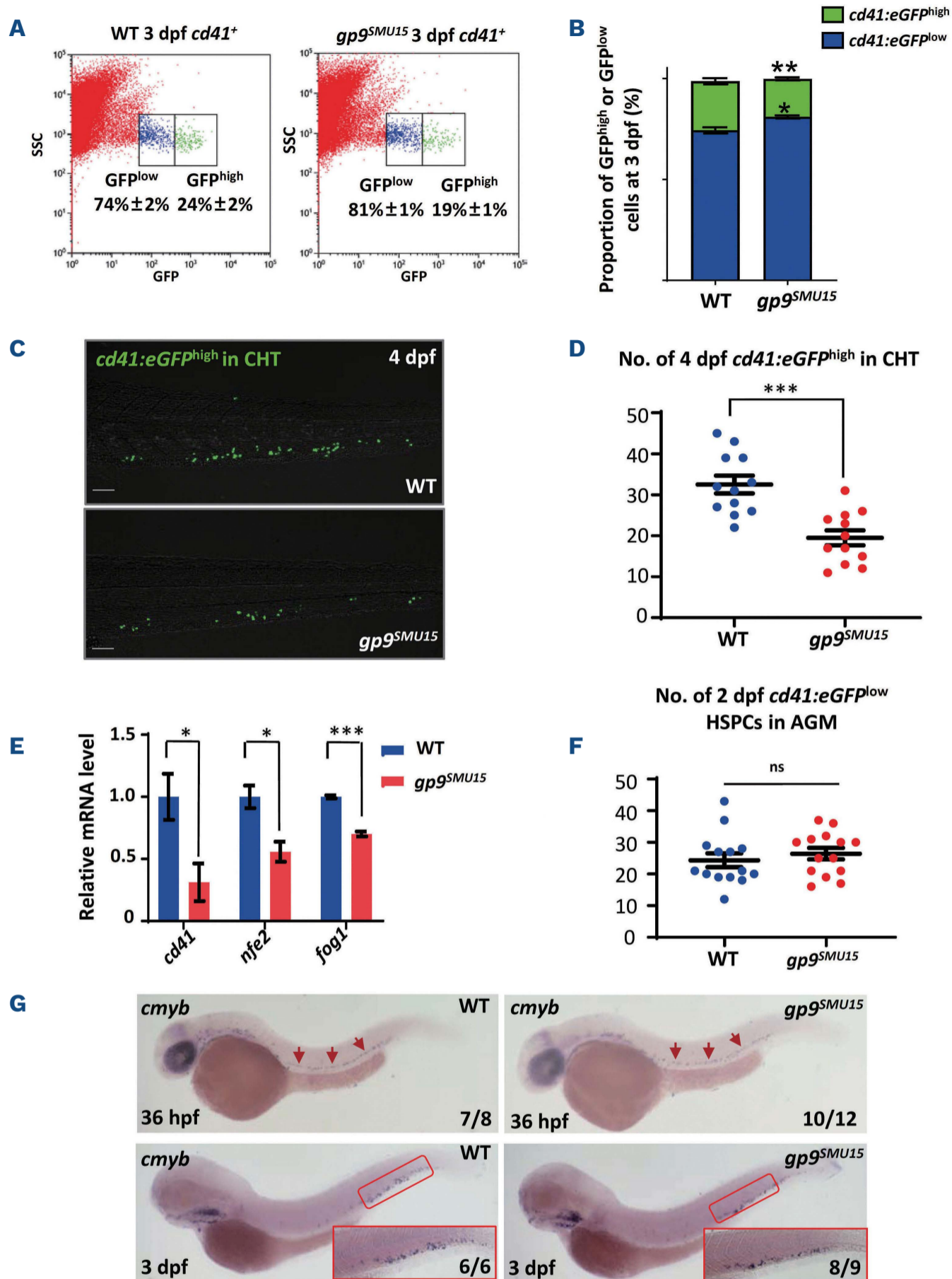


Figure 4. Thrombocytopenia in *gp9*^{SMU15} zebrafish embryos. (A–D) *cd41:eGFP*^{high} thrombocytes were decreased in *gp9*^{SMU15} embryos. Flow cytometry analysis of *cd41:eGFP*⁺ cells in 3-day post fertilization (dpf) wild-type (WT) and *gp9*^{SMU15} embryos. GFP area was directly proportional to 488-GFP cells and side scatter (SSC) was indicative of cellular granularity (A). Percentage of *cd41:eGFP*^{low} and *cd41:eGFP*^{high} thrombocytes in 3-dpf embryo cells determined by flow cytometry (Student *t*-test, *n*>100 embryos per group, and data were combined from three biological replicates, mean ± standard error of mean [SEM], ns: not significant, ***P*<0.01) (B). Representative images for staining of *cd41:eGFP* protein in 4 dpf *Tg(cd41:eGFP)*^{WT} and mutant *Tg(cd41:eGFP);gp9*^{SMU15} embryos. Images showed *GFP*^{high} signals (C). Statistical significance was determined using a two-sample Student *t*-test, *n*>10, mean ± SEM, ****P*<0.001 (D). (E) Relative expressions of thrombocytic markers (*cd41*, *nfe2* and *fog1*) in 3-dpf WT siblings (blue column) and *gp9*^{SMU15} mutants (red column) by quantitative real-time polymerase chain reaction. Statistical significance was determined using a two-sample Student *t*-test; *n*≥10 per group, and data were combined from three biological replicates, mean ± SEM, **P*<0.05, ****P*<0.001. (F) Hematopoietic stem and progenitor cells (HSPC) were not affected in *gp9*^{SMU15} mutants. Quantification of the aorta-gonad-mesonephros (AGM)-localized *cd41:eGFP*^{low} HSPC in *gp9*^{SMU15} mutants and WT embryos at 2 dpf. Statistical significance was determined using a two-sample Student *t*-test, *n*>10, mean ± SEM, ns: not significant. (G) Whole-mount *in situ* hybridization (WISH) of *cmyb* expression in control (left panel) and *gp9*^{SMU15} (right panel) embryos at 36 hours post fertilization (hpf) and 3 dpf.

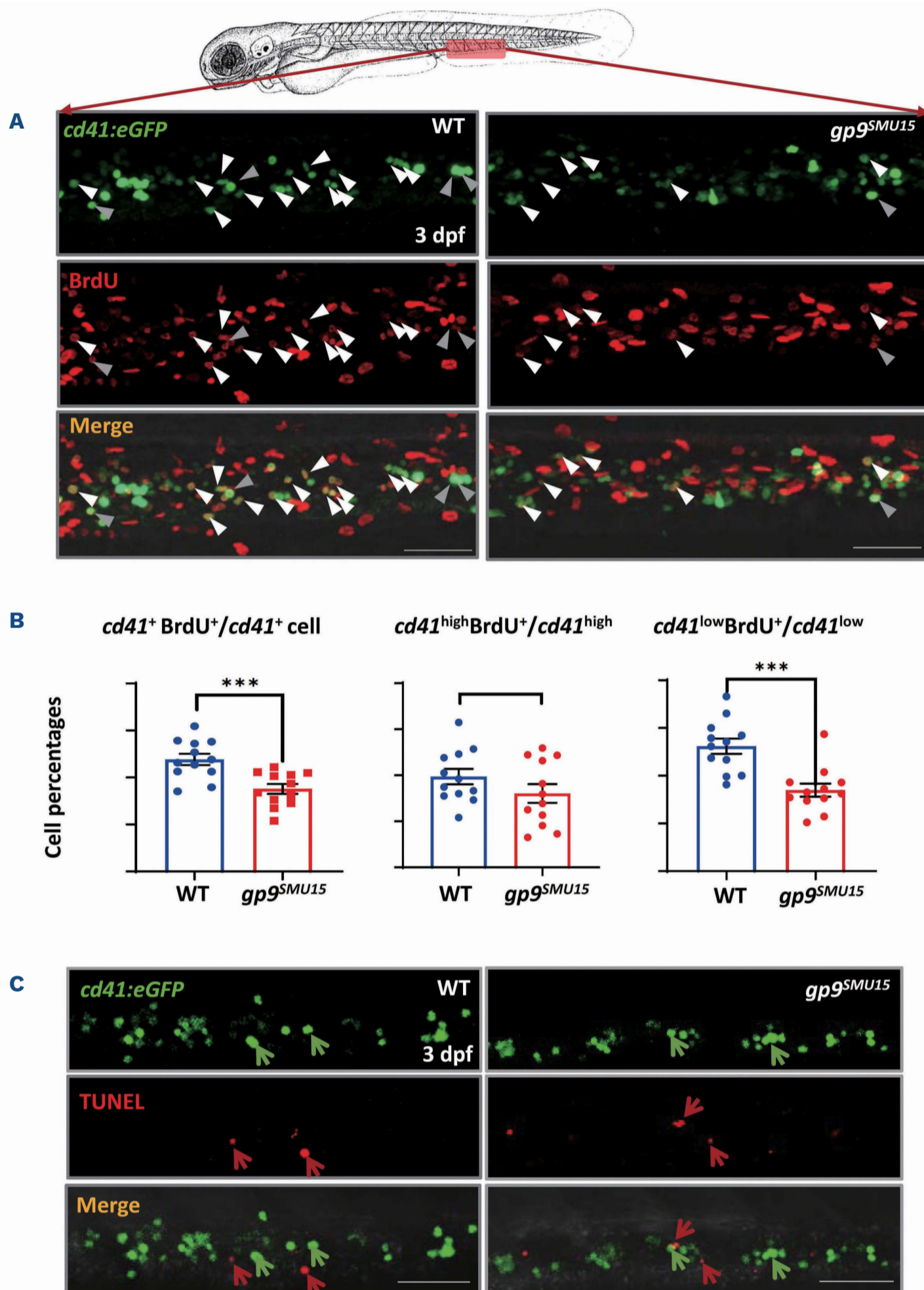


Figure 5. Abated thrombocyte precursor proliferation in *gp9^{SMU15}* mutants. (A) Profiling of BrdU incorporation by caudal hematopoietic tissue (CHT) *cd41:eGFP⁺* cells in 3-day post-fertilization (dpf) *Tg(cd41:eGFP);^{WT}* (left) and *Tg(cd41:eGFP);gp9^{SMU15}* (right) by double antibody staining of BrdU (red signals) and GFP (green signals). White triangular arrowheads indicate the yellow color merged signals represent the *BrdU⁺cd41^{low}* cells. Gray triangular arrowheads indicate the yellow color merged signals represent the *BrdU⁺cd41^{high}* cells. The images of the stained samples were captured by setting the confocal parameter as pinhole size 35 μm and 488 laser gain 700 to filter most *cd41:eGFP^{low}* signals, and the *cd41:eGFP^{high}* thrombocytes fluorescent signals were counted. Scale bars: 50 μm . (B) Statistical data showing the percentages of CHT-localized *cd41:eGFP⁺* cells that incorporated BrdU. Asterisks indicate statistical difference, determined using a two-sample Student *t*-test, $n \geq 10$, mean \pm standard error of mean, $**P < 0.01$. (C) No TUNEL incorporation with 3-dpf *cd41:eGFP⁺* cells in the CHT of *Tg(cd41:eGFP);gp9^{SMU15}* mutants (right panels) and their wild-type (WT) siblings (left panels). Green: GFP; red: TUNEL. The green arrowheads indicate the *cd41:eGFP⁺* cells and the red arrowheads indicate the TUNEL+ cells, No *cd41:eGFP⁺/TUNEL⁺* cells were detected. Scale bars: 50 μm .

in $gp9^{SMU15}$ zebrafish embryos to evaluate the function of the two isoforms on thrombocytopoiesis. Unlike $hsGP9^{WT}$ overexpression, $hsGP9^{70T>C}$ and $hsGP9^{182A>G}$ overexpression did not restore $cd41:eGFP^{high}$ thrombocyte counts in $gp9^{SMU15}$ mutants (Figure 6B, C), suggesting that two human GP9 mutations affect GP9 function on thrombocytopoiesis. The above data demonstrate that the $gp9^{SMU15}$ zebrafish model could serve as a good BSS model for functional validation of human GP9 mutations, and that $hsGP9^{70T>C}$ and $hsGP9^{182A>G}$ are both loss-of-function mutations.

Thrombopoietin and decitabine effectively modify Bernard-Soulier syndrome phenotypes in the model

In clinical settings, the primary treatment for BSS is bone marrow transplantation. Since BSS patients show symp-

toms of thrombocytopenia, we wondered whether drugs clinically used for the treatment of thrombocytopenia would be effective to relieve BSS. We therefore utilized the $Tg(cd41:eGFP);gp9^{SMU15}$ BSS zebrafish to test drug responses. rhTPO is a commercially available thrombopoietic agent approved by the US Food and Drug Administration (FDA) for the treatment of human thrombocytopenia.³⁹ We treated 1.5-dpf WT sibling embryos with rhTPO until 4 dpf to see whether zebrafish thrombocytes could respond to rhTPO (Figure 7A) and found that 100 U/mL rhTPO could effectively increase $cd41:eGFP^{high}$ thrombocyte numbers in both WT sibling embryos and $gp9$ -deficient mutants. This suggested a conserved response from zebrafish thrombocytes to mammalian cytokines, and that rhTPO could relieve thrombocytopenia in BSS fish (Figure 7B, C).

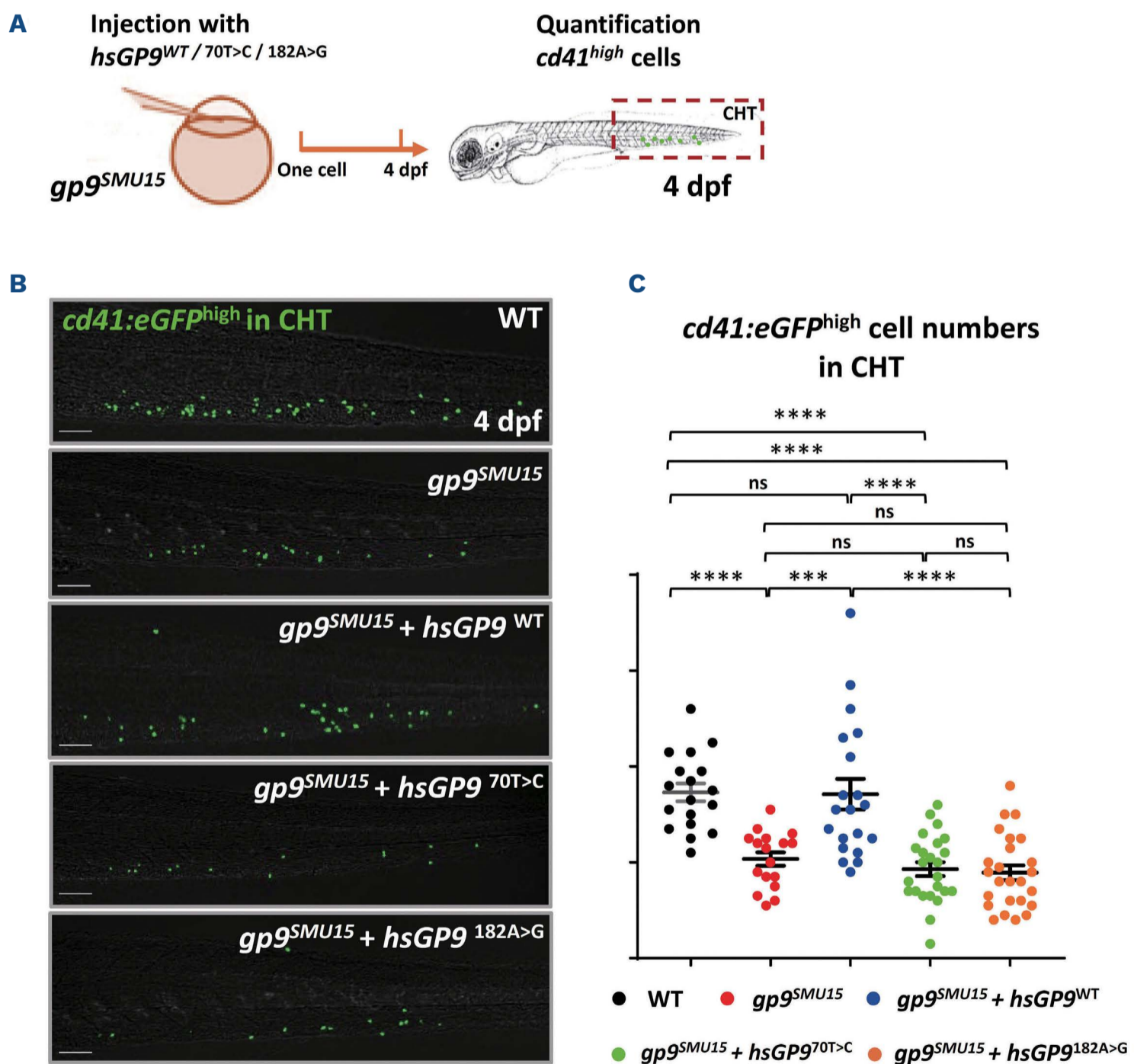


Figure 6. Functional validations of the human-derived GP9 mutations associated with Bernard-Soulier syndrome in the $gp9^{SMU15}$ zebrafish model. (A) Schematic diagram of the validation of the Bernard-Soulier syndrome (BSS) zebrafish model using human BSS-related GP9 mutations. $hsGP9^{WT}$, $hsGP9^{70T>C}$ and $hsGP9^{182A>G}$ mRNA were injected into one cell of the $Tg(cd41:eGFP);gp9^{SMU15}$ embryos. (B) Representative images of staining of $cd41:eGFP$ protein in 4 days post-fertilization (dpf) $Tg(cd41:eGFP);WT$ and mutant $Tg(cd41:eGFP);gp9^{SMU15}$ embryos. Images show GFP^{high} signals. (C) Quantification of GFP^{high} cell numbers at the caudal hematopoietic tissue (CHT) region. Statistical significance was determined by a Student t -test, $n > 10$, mean \pm SEM, *** $P < 0.001$, **** $P < 0.0001$. Scale bars: 50 μ m.

Decitabine, approved by the FDA for the treatment of leukemia and myelodysplastic syndrome,³⁶ is now being used for the treatment of idiopathic thrombocytopenia purpura in clinical trials.³⁷ Whether it could be used to treat BSS is unknown. We found that 20 μM decitabine could effectively increase $cd41:eGFP^{\text{high}}$ thrombocytes in WT sibling embryos, and also expand thrombocytes in $gp9^{\text{SMU15}}$ embryos (Figure 7D, E), suggesting that decitabine

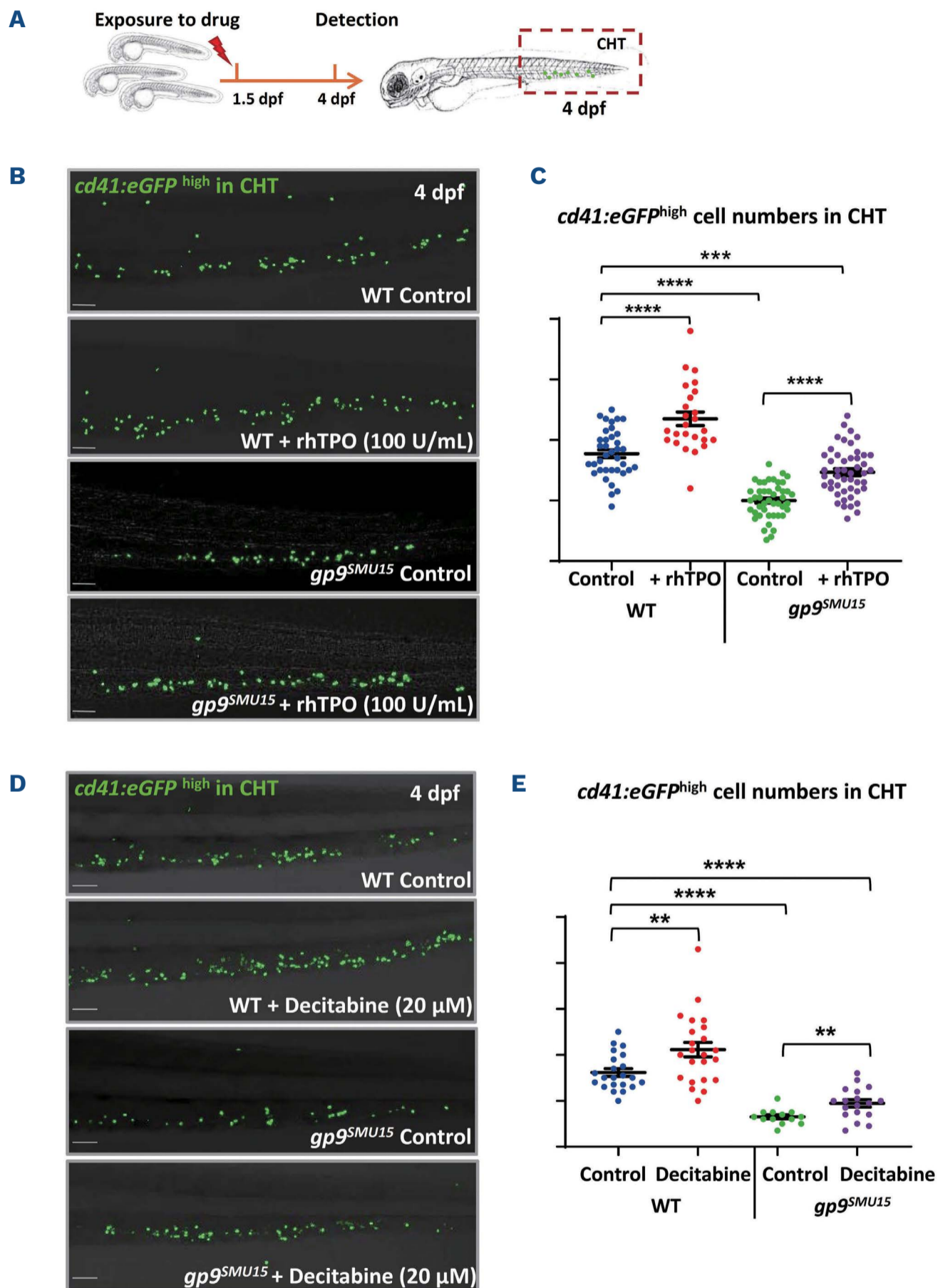


Figure 7. Therapeutic responses of $Tg(cd41:eGFP);gp9^{\text{SMU15}}$. (A) Schematic diagram of the drug treatment. The embryos were exposed to recombinant human thrombopoietin (rhTPO) and decitabine at 1.5 days post-fertilization (dpf) and fixed at 4 dpf. (B) Thrombocytopenia indicated by decreased $cd41:eGFP^{\text{high}}$ cells in $Tg(cd41:eGFP);gp9^{\text{SMU15}}$ mutant embryos and thrombocyte expansion by rhTPO. Images show GFP^{high} signals. Representative images of $Tg(cd41:eGFP);WT$ and $Tg(cd41:eGFP);gp9^{\text{SMU15}}$ embryos treated with sodium chloride saline control and rhTPO (B). (C) Statistical significance was determined using a paired Student t -test, $n \geq 5$, mean \pm standard error of mean (SEM), * $P < 0.05$, ** $P < 0.01$, *** $P < 0.001$, **** $P < 0.0001$. (D) Representative images of $Tg(cd41:eGFP);WT$ and $Tg(cd41:eGFP);gp9^{\text{SMU15}}$ embryos treated with dimethylsulfoxide (DMSO) control and decitabine. Images show GFP^{high} signals. (E) Quantification of $cd41:eGFP^{\text{high}}$ numbers in the caudal hematopoietic tissue (CHT). Statistical significance was determined by a paired Student t -test, $n > 10$, mean \pm SEM. * $P < 0.05$, ** $P < 0.01$, *** $P < 0.001$, **** $P < 0.0001$. Scale bars: 50 μm .

could increase the number of zebrafish thrombocytes and may relieve thrombocytopenia in the BSS model. The above results demonstrate that both rhTPO and decitabine could effectively relieve thrombocytopenia in BSS zebrafish (although thrombocyte numbers were not fully rescued), suggesting that these drugs, clinically used for thrombocytopenia, could also be applied in the treatment of BSS. The response of the BSS zebrafish model to these therapeutic agents suggests that the model could be useful for the evaluation and screening of thrombopoietic drugs.

Discussion

BSS, characterized by prolonged bleeding times, enlarged platelets, an inability to clot and thrombocytopenia, are bleeding disorders that result from mutations in genes of the glycoprotein Ib complex, including *GP1bA*, *GP1bB* and *GP9*.¹⁰ *GP9* in particular is the most frequently mutated gene reported in a group of BSS patients from 211 families.¹⁰ In this study, we generated and characterized a CRISPR-Cas9 targeted *gp9*^{SMU15} zebrafish mutant, which is the first established inherited BSS zebrafish model. The *gp9*-deficient zebrafish were viable and displayed thrombocytopenia, with a bleeding disorder, thus resembling *Gp9*-knockout mice and human BSS patients. The *gp9*^{SMU15} zebrafish mutant provides a complementary model to aid our understanding of the various roles of *gp9* in thrombocytopoiesis and in BSS. Thrombocytopenia is an important feature reported in both human BSS and *Gp9* knockout mice. Our data strengthened our understanding of the role of *gp9* in thrombocytopoiesis in vertebrates, as *gp9*-deficient zebrafish showed a consistent thrombocytopenia phenotype from embryonic stages to adulthood. We also demonstrated that *gp9*^{SMU15} zebrafish showed reduced thrombocytes but increased precursor cells from embryonic to adult stages. Interestingly, the 3 dpf whole-mount *in situ* hybridization showed unaltered *cmyb* expression but *cd41:eGFP*^{low} cells were increased, suggesting that the increased *cd41:eGFP*^{low} cells were likely thrombocyte-erythroid progenitors rather than *cmyb*⁺ hematopoietic stem cells or other lineage progenitors. In particular, their KM *cd41:eGFP*⁺ cells were larger than their siblings, similar to the larger thrombocytic cell volumes in mice and humans.^{9,16} As regards the cellular mechanisms for the thrombocytopenia caused by *gp9* mutations, we further clarified that thrombocytopenia may be attributed to proliferation defects in thrombocyte lineage cells. It is probable that proliferation blocked precursors or thrombocyte progenitors had consequent problems in differentiating into thrombocytes.

Thrombocytes in zebrafish are the functional equivalent of mammalian platelets, playing major roles in clotting and preventing bleeding.¹⁸ Patients with thrombocytopenia or

bleeding disorders can have severe hemorrhage following injury or surgery. Similarly to BSS patients, *gp9*-deficient zebrafish also display a spontaneous bleeding syndrome, accompanied by a prolonged bleeding time after injury. Taken together, these results confirm that *gp9* deficiency increases the tendency to bleeding, which is conserved from zebrafish to humans. The bleeding disorders in *gp9*-deficient animals and patients could be attributed to insufficiently functional thrombocytes. The activation of thrombocytes may also be affected in *GP9*-mutated individuals, according to several reports.^{38,39} Taken together, these results suggested that zebrafish with inherited *gp9*-deficiency, displaying a bleeding disorder resembling human BSS, could serve as a complementary model to broaden our understanding of the various roles of *GP9* in thrombocytopoiesis, as well as in thrombosis and hemostasis.

Based on the conservation of thrombocytopoiesis regulatory factors and strong similarity of GPIX across species, we verified that human *GP9* could compensate zebrafish *gp9*, as human *GP9*^{WT} mRNA is able to rescue thrombocytopenia in *gp9*^{SMU15} zebrafish. For functional validation of the BSS patient-derived mutations, previous studies were mainly restricted to cell lines.^{40,41} Here we provide an example of fast verification of patient-derived mutations using zebrafish, as we showed that *gp9*^{SMU15} zebrafish could serve as a cost-effective model for validating human *GP9* mutations associated with BSS. The two *GP9* mutations (*hsGP9*^{70T>C} and *hsGP9*^{182A>G}) associated with BSS were evaluated by simply overexpressing them in the zebrafish model, and the failure to rescue thrombocytopenia confirmed that the two mutations are loss-of-function mutations in thrombocytopoiesis. Thus, the BSS zebrafish model with a high-throughput screening capability could help to accelerate the discovery of potential genetic variants of unknown clinical significance *in vivo*.

The primary clinical treatment for BSS is supportive with platelet transfusions, anti-fibrinolytics particularly for mucocutaneous bleeds and recombinant activated factor VII in attempts to shorten bleeding times.⁴²⁻⁴⁴ More effective ways to treat BSS are much needed. Previous studies have shown that rhTPO rapidly increases platelet counts in patients with idiopathic thrombocytopenia purpura,⁴⁵ and low-dose decitabine promotes thrombocytopoiesis in idiopathic thrombocytopenia purpura and healthy controls.⁴⁶ Here, we showed that rhTPO and decitabine could efficiently relieve BSS phenotypes in zebrafish larvae (Figure 7). Given that the thrombocytopenia deficiency could be consistently observed in both larval and adult stages of zebrafish (Figures 2 and 4), we think that the two drugs may still relieve thrombocytopenia in adult BSS zebrafish if administered at a proper dose using a suitable way of drug delivery. The BSS zebrafish model will be beneficial for drug discovery, as evidenced by the demonstration that rhTPO and decitabine,

used for promoting thrombocytopoiesis, also effectively relieved BSS phenotypes in the zebrafish larvae, which may also shed light on the treatment of BSS by promoting thrombocytopoiesis.

In summary, we established a *gp9*-deficient zebrafish model displaying thrombocytopenia and a bleeding disorder, which resemble the clinical features of BSS in patients. We confirmed the conservation of the roles of *GP9* in thrombocytopoiesis as well as in thrombosis and hemostasis from zebrafish to mammals. The BSS zebrafish model could be utilized as a cost-effective model to evaluate the function of human related mutations, and this line may also be applied in *in vivo* screening for novel drugs to treat BSS. The zebrafish BSS model, as a proof-of-principle example, together with other established thrombocyte related zebrafish models, will allow us to examine the effect of clinically discovered mutations with uncertain clinical significance in thrombocyte development and function, as well as to conduct a robust drug evaluation or establish a screening platform to assess the therapeutic response of BSS, particularly against mutations with thrombocytopenia.

Disclosures

No conflicts of interest to disclose.

References

- Nakao K, Angrist AA. Membrane surface specialization of blood platelet and megakaryocyte. *Nature*. 1968;217(5132):960-961.
- Lordier L, Jalil A, Aurade F, et al. Megakaryocyte endomitosis is a failure of late cytokinesis related to defects in the contractile ring and Rho/Rock signaling. *Blood*. 2008;112(8):3164-3174.
- Machlus KR, Italiano JJ. The incredible journey: from megakaryocyte development to platelet formation. *J Cell Biol*. 2013; 201(6):785-796.
- Woolthuis CM, Park CY. Hematopoietic stem/progenitor cell commitment to the megakaryocyte lineage. *Blood*. 2016;127(10):1242-1248.
- Bianchi E, Norfo R, Pennucci V, Zini R, Manfredini R. Genomic landscape of megakaryopoiesis and platelet function defects. *Blood*. 2016;127(10):1249.
- Lanza F. Bernard-Soulier syndrome (hemorrhagic thrombocytopenic dystrophy). *Orphanet J Rare Dis*. 2006;1:46.
- Bernard J, Soulier JP. Sur une nouvelle variété de dystrophie thrombocytaire-hémorragique congénitale. *Sem Hop Paris*. 1948;24(Spec. No.):3217-3222
- de la Salle C, Lanza F, Cazenave JP. Biochemical and molecular basis of Bernard-Soulier syndrome: a review. *Nouv Rev Fr Hematol*. 1995;37(4):215.
- Lopez J, Andrews R, Afshar-Kharghan V, Berndt M. Bernard-Soulier syndrome. *Blood*. 1998;91:4397-4418.
- Savoia A, Kunishima S, De Rocco D, et al. Spectrum of the mutations in Bernard-Soulier syndrome. *Hum Mutat*. 2014;35(9):1033-1045.
- McEwan PA, Yang W, Carr KH, et al. Quaternary organization of GPIb-IX complex and insights into Bernard-Soulier syndrome revealed by the structures of GPIb β and a GPIb β /GPIX chimera. *Blood*. 2011;118(19):5292-5301.
- Clemetson JM, Kyrle PA, Brenner B, Clemetson KJ. Variant Bernard-Soulier syndrome associated with a homozygous mutation in the leucine-rich domain of glycoprotein IX. *Blood*. 1994;84(4):1124-1131.
- Rivera CE, Villagra J, Riordan M, Williams S, Lindstrom KJ, Rick ME. Identification of a new mutation in platelet glycoprotein IX (GPIX) in a patient with Bernard-Soulier syndrome. *Br J Haematol*. 2001;112(1):105-108.
- Dagistan N, Kunishima S. First Turkish case of Bernard-Soulier syndrome associated with GPIX N45S. *Acta Haematol*. 2007;118(3):146-148.
- Ali S, Ghosh K, Shetty S. Novel genetic abnormalities in Bernard-Soulier syndrome in India. *Ann Hematol*. 2014;93(3):381-384.
- Meehan TF, Conte N, West DB, et al. Disease model discovery from 3,328 gene knockouts by The International Mouse Phenotyping Consortium. *Nat Genet*. 2017; 49(8):1231-1238.
- Jagadeeswaran P, Liu YC, Sheehan JP. Analysis of hemostasis in the zebrafish. *Methods Cell Biol*. 1999;59:337-357.
- Jagadeeswaran P, Sheehan JP, Craig FE, Troyer D. Identification and characterization of zebrafish thrombocytes. *Br J Haematol*. 1999;107(4):731-738.
- Lin H-F, Traver D, Zhu H, et al. Analysis of thrombocyte development in CD41-GFP transgenic zebrafish. *Blood*. 2005;106(12):3803-3810.
- Khandekar G, Kim S, Jagadeeswaran P. Zebrafish thrombocytes: functions and origins. *Adv Hematol*. 2012;2012:857058.
- Lin Q, Zhang Y, Zhou R, et al. Establishment of a congenital amegakaryocytic thrombocytopenia model and a thrombocyte-

Contributions

YZ conceived and supervised the study and wrote, reviewed and edited the article; QL conceived the study, performed investigations and wrote, reviewed and edited the article; RZ and PM performed investigations, wrote, reviewed and edited the article; LW, LY, WL, JW, YC and LS performed investigations, analyzed the data and wrote the original draft of the manuscript.

Acknowledgments

The authors thank Dr. Jin Xu for his constructive suggestions and Mr. Xiaohui Chen for helping with the maintenance of zebrafish lines.

Funding

This work was supported by the National Natural Science Foundation of China (81870100 and 31871475), the National Key R&D Program of China (2018YFA0800200), Guangdong Province Universities and Colleges Pearl River Scholar Funded Scheme (2019), and Fundamental Research Funds for the Central Universities (2019ZD54 and 2018MS69).

Data-sharing statement

The data supporting the findings of this study are available within the article and its supplementary material.

- specific reporter line in zebrafish. *Leukemia*. 2017;31(5):1206-1216.
22. Rost MS, Shestopalov I, Liu Y, et al. Nfe2 is dispensable for early but required for adult thrombocyte formation and function in zebrafish. *Blood Adv*. 2018;2(23):3418-3427.
 23. Marconi C, Di Buduo CA, LeVine K, et al. Loss-of-function mutations in PTPRJ cause a new form of inherited thrombocytopenia. *Blood*. 2019;133(12):1346-1357.
 24. Ma AC, Cheung AM, Ward AC, et al. The study of Jak2 V617F mutation in polycythemia vera with zebrafish model. *Cell Res*. 2008;18(S1):S141-S141.
 25. Albers CA, Cvejic A, Favier R, et al. Exome sequencing identifies NBEAL2 as the causative gene for gray platelet syndrome. *Nat Genet*. 2011;43(8):735-737.
 26. Gregory M, Hanumanthaiah R, Jagadeeswaran P. Genetic analysis of hemostasis and thrombosis using vascular occlusion. *Blood Cells Mol Dis*. 2002;29(3):286-295.
 27. Kim S, Carrillo M, Kulkarni V, Jagadeeswaran P. Evolution of primary hemostasis in early vertebrates. *PLoS One*. 2009;4(12):e8403.
 28. Deebani A, Iyer N, Raman R, Jagadeeswaran P. Effect of MS222 on hemostasis in zebrafish. *J Am Assoc Lab Anim Sci*. 2019;58(3):390-396.
 29. Zheng L, Abdelgawwad MS, Zhang D, et al. Histone-induced thrombotic thrombocytopenic purpura in adamts13^{-/-} zebrafish depends on von Willebrand factor. *Haematologica*. 2020;105(4):1107-1119.
 30. Macaulay IC, Svensson V, Labalette C, et al. Single-cell RNA-sequencing reveals a continuous spectrum of differentiation in hematopoietic Cells. *Cell Rep*. 2016;14(4):966-977.
 31. Ma D, Zhang J, Lin HF, Italiano J, Handin RI. The identification and characterization of zebrafish hematopoietic stem cells. *Blood*. 2011;118(2):289-297.
 32. Svoboda O, Stachura DL, Machoňová O, et al. Dissection of vertebrate hematopoiesis using zebrafish thrombopoietin. *Blood*. 2014;124(2):220-228.
 33. Savoia A, Pastore A, De Rocco D, et al. Clinical and genetic aspects of Bernard-Soulier syndrome: searching for genotype/phenotype correlations. *Haematologica*. 2011;96(3):417-423.
 34. Kissa K, Murayama E, Zapata A, et al. Live imaging of emerging hematopoietic stem cells and early thymus colonization. *Blood*. 2008;111(3):1147-1156.
 35. Mo X, Nguyen NX, Mcewan PA, et al. Binding of platelet glycoprotein Ib β through the convex surface of leucine-rich repeats domain of glycoprotein IX. *J Thromb Haemost*. 2009;7(9):1533-1540.
 36. Jabbour E, Issa JP, Garcia-Manero G, Kantarjian H. Evolution of decitabine development: accomplishments, ongoing investigations, and future strategies. *Cancer*. 2008;112(11):2341-2351.
 37. Zhou H, Qin P, Liu Q, et al. A prospective, multicenter study of low dose decitabine in adult patients with refractory immune thrombocytopenia. *Am J Hematol*. 2019;94(12):1374-1381.
 38. Michelson AD, Benoit SE, Furman MI, Barnard MR, Nurden P, Nurden AT. The platelet surface expression of glycoprotein V is regulated by two independent mechanisms: proteolysis and a reversible cytoskeletal-mediated redistribution to the surface-connected canalicular system. *Blood*. 1996;87(4):1396-1408.
 39. Canobbio I, Balduini C, Torti M. Signalling through the platelet glycoprotein Ib-V-IX complex. *Cell Signal*. 2004;16(12):1329-1344.
 40. Zmajkovic J, Lundberg P, Nienhold R, et al. A gain-of-function mutation in EPO in familial erythrocytosis. *N Engl J Med*. 2018;378(10):924-930.
 41. Kim AR, Ulirsch JC, Wilmes S, et al. Functional selectivity in cytokine signaling revealed through a pathogenic EPO mutation. *Cell*. 2017;168(6):1053.
 42. Grainger JD, Thachil J, Will AM. How we treat the platelet glycoprotein defects; Glanzmann thrombasthenia and Bernard Soulier syndrome in children and adults. *Br J Haematol*. 2018;182(5):621-632.
 43. Almeida AM, Khair K, Hann I, Liesner R. The use of recombinant factor VIIa in children with inherited platelet function disorders. *Br J Haematol*. 2003;121(3):477-481.
 44. Ozelo MC, Svirin P, Larina L. Use of recombinant factor VIIa in the management of severe bleeding episodes in patients with Bernard-Soulier syndrome. *Ann Hematol*. 2005;84(12):816-822.
 45. Wang S, Yang R, Zou P, et al. A multicenter randomized controlled trial of recombinant human thrombopoietin treatment in patients with primary immune thrombocytopenia. *Int J Hematol*. 2012;96(2):222-228.
 46. Zhou H, Hou Y, Liu X, et al. Low-dose decitabine promotes megakaryocyte maturation and platelet production in healthy controls and immune thrombocytopenia. *Thromb Haemost*. 2015;113(5):1021-1034.